Available online at www.sciencedirect.com

ScienceDirect

IFAC PapersOnline CONFERENCE PAPER ARCHIVE

IFAC PapersOnLine 53-2 (2020) 12479–12484

Nonlinear State and Parameter Estimation for Li-ion Batteries with Thermal Coupling

Dong Zhang * **Luis D. Couto** ** **Saehong Park** * **Preet Gill** * **Scott J. Moura** *

* *Department of Civil and Environmental Engineering, University of California at Berkeley, CA 94720, USA (e-mail: {dongzhr,sspark,preetgill77,smoura}@ berkeley.edu).*

** *Department of Control Engineering and System Analysis, Université libre de Bruxelles, B-1050 Brussels, Belgium (e-mail: lcoutome@ulb.ac.be).*

Abstract: Advanced Lithium-ion battery management systems rely on accurate cell-level state of charge (SOC) and parameter estimation for safe and efficient real-time monitoring. However, the design of combined state and parameter estimators that are provably convergent is notoriously difficult. A robust observer framework based on a coupled equivalent circuit-thermal model for a cylindrical battery is proposed. The coupled model also takes into account SOC and temperature-dependent electrical parameters for higher accuracy. In the literature, the model parameters are often treated as constants to simplify model structure and observer analysis. The problem considered in this work is particularly challenging due to (i) nonlinear two-way coupling between electrical and thermal sub-models, and (ii) nonlinear dependence of model parameters on the system states. A single aggregated observer for both SOC and thermal estimation becomes intractable due to lack of convergence certification caused by complex model coupling. We tackle this problem by proposing a sequential estimation scheme such that every sub-estimator converges separately, which is mathematically verified by Lyapunov stability analysis. Simulation results demonstrate the performance of the proposed state and parameters estimation framework.

Keywords: Li-ion Battery, State Estimation, Thermal Coupling, Lyapunov Stability, Robust Estimation, State-Dependent Parameters.

1. INTRODUCTION

From mobile phones to electric vehicles, Lithium-ion (Li-ion) batteries are the energy storage technology that make these applications viable due to their high energy density, low self-discharge rate, and high efficiency (Chaturvedi et al., 2010). To extract their full potential while ensuring safety, the internal states of Li-ion batteries need to be properly monitored. Particularly relevant states are the state of charge (SOC) and internal temperature. The former is the fuel gauge of the battery, whereas the latter directly impacts battery health and safety. Neither of them are directly measured, and only nonlinear transformations of them can be accessed through voltage and surface temperature measurements during regular operation.

The model-based estimation problem of Li-ion batteries has been widely considered in the literature. Interested readers may refer to Pop et al. (2005); Hannan et al. (2017). The estimation methods can be divided depending of the type of model used, namely data-driven models, physical models, and equivalent circuit models (ECM) (Zhang et al., 2017; Park et al., 2017). The first model type is black box and it suffers from needing a large training data set to describe the nonlinear behavior of the battery. The second model type benefits from its physical transparency (Zhang et al., 2019a), but the resulting models are complex to run online and its parameters might not be identifiable. In this context, the last model type constitutes a good compromise between prediction accuracy and computational complexity (Hu et al., 2012). Given that electrical parameters are known to change with operating conditions (Wang et al., 2017), ECMs have been extended to form coupled equivalent circuit-thermal models as well as models with SOC-dependent parameters (Lin et al., 2014).

For the ECM model-based estimation, two main paths can be distinguished, namely stochastic filtering and nonlinear observers. The most prolific contribution in the first approach has been variants of Kalman filters (KF) (Plett, 2004). Some approaches assume constant and known parameters (Rahimi-Eichi et al., 2013), or unknown slowly time-varying parameters that are estimated alongside the states via joint/dual estimation (Wang et al., 2017; Restaino and Zamboni, 2012). Others take into account SOC-dependent parameters by relying on robust observers (Lotfi and Landers, 2012). Ouyang et al. (2014) reported an observer for SOC and temperature subject to state-dependent parametric changes. However,

⋆ Luis D. Couto would like to thank the Wiener-Anspach Foundation for its financial support.

10.1016/j.ifacol.2020.12.1752

the coupling between the electrical and thermal models is ignored, which eases the observer design at the sacrifice of model fidelity. Aside from the limited amount of work, most approaches covering state-dependent parameters resort to nonlinear KFs. Additionally, adaptive observers exploit SOC-dependent/temperature-compensated models and combine the state observer with parameter estimators, e.g. Least-Squares (Rahimi-Eichi et al., 2013) or Lyapunov-based estimators (Ning et al., 2016).

Battery model parameters are well-known to fluctuate with SOC, temperature, and aging (Wang et al., 2017; Meng et al., 2018), and the literature has not appropriately addressed the state observer design considering explicit two-way coupling in electro-thermal model [1]. In light of the aforementioned challenge and existing work, this paper contributes to the existing literature in the following ways:

- Designing an adaptive observer for combined state (SOC and internal temperature) and parameter estimation based on an ECM with thermal coupling;
- Proposing a nonlinear observer in a sequential fashion to account for state-dependent electrical parameters, which makes tractable the convergence analysis for the estimators compared to aggregated ones.

2. MODEL DEVELOPMENT

This section reviews a two-way coupled electro-thermal model that consists of an equivalent-circuit model and a two-state thermal model for a cylindrical battery cell.

The ECM for a battery cell, shown in Fig. 1, is described by the following continuous-time dynamical equations,

$$\dot{z}(t) = \frac{1}{Q} I(t), \tag{1}$$

$$\dot{V}_c(t) = -\frac{V_c(t)}{R_2(z,T,\eta)C(z,T,\eta)} + \frac{I(t)}{C(z,T,\eta)}, \tag{2}$$

$$V(t) = V_{oc}(z(t)) + V_c(t) + R_1(z,T,\eta)I(t), \tag{3}$$

where $z(t)$ represents the cell SOC, $V_c(t)$ denotes the voltage across the R-C circuit, and $I(t)$ is the applied current. We herein specify positive current for charging and negative current for discharging. Battery charge capacity is denoted by Q. $T(t)$ represents the cell temperature. The electrical model parameters, namely R_1, R_2, and C, are dependent on cell SOC, temperature, and the sign of current $\eta \in \{+, -\}$. Such dependence can be explicitly characterized via an offline experiment. For instance, the work by Lin et al. (2014) on a $LiFePO_4$/Graphite cell conducted a set of experiments at various SOC and temperature points, and proposed empirical equations used to predict parameter values. The output equation (3) provides the voltage response determined by a nonlinear open circuit voltage (OCV) as a function of SOC, voltage from the R-C pair, and voltage associated with resistance R_1.

A two-state thermal model is adopted from Lin et al. (2014). The model states are cell core temperature and surface temperature:

[1] The phrase "two-way coupling" indicates that the electrical and thermal sub-models have explicit influence on each other.

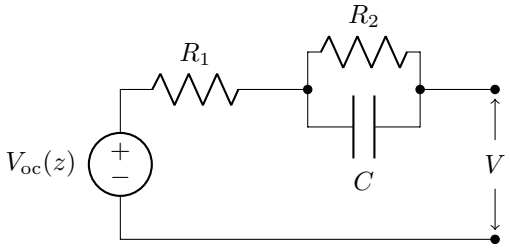

Fig. 1. The schematic of an equivalent circuit model

$$C_c \frac{dT_c(t)}{dt} = \frac{T_s(t) - T_c(t)}{R_c} + E(t) \tag{4}$$

$$C_s \frac{dT_s(t)}{dt} = \frac{T_f(t) - T_s(t)}{R_u} - \frac{T_s(t) - T_c(t)}{R_c} \tag{5}$$

$$E(t) = I(t)\left[V(t) - V_{oc}(z(t))\right], \tag{6}$$

$$T(t) = \frac{1}{2}\left(T_s(t) + T_c(t)\right), \tag{7}$$

where $T_c(t)$ and $T_s(t)$ denote core and surface temperatures, and $T(t)$ represents the average between core and surface. Symbols R_c, R_u, C_c, and C_s represent heat conduction resistance between core and surface, convection resistance between ambient and surface, core heat capacity, and surface heat capacity, respectively. Symbol $E(t) \geq 0$ represents the internal heat generation from resistive dissipation. Note that the electrical model (1)-(3) and the thermal model (4)-(7) are non-linearly coupled via

(1) internal heat generation $E(t)$, since $E(t)$ explicitly depends on $z(t)$ generated by the electrical model;
(2) thermally-dependent electrical parameters, namely $R_1(z,T,\eta)$, $R_2(z,T,\eta)$, and $C(z,T,\eta)$.

The measured quantities for the coupled electro-thermal model (1)-(7) are the cell voltage and surface temperature:

$$y(t) = \left[V(t), T_s(t)\right]^\top. \tag{8}$$

3. ESTIMATION WITH CONSTANT PARAMETERS

As an intermediate step, suppose the state-dependent electrical parameters in (2)-(3) are constants, and each takes a nominal value, i.e. $R_1(z,T,\eta) = R_1^0$, $R_2(z,T,\eta) = R_2^0$, and $C(z,T,\eta) = C^0$. We refer to this model as the "reduced model". The objective of this section is to design an adaptive observer to estimate the states (SOC and core temperature) as well as the constant electrical parameters in the reduced model in an online fashion.

It is worth highlighting that the reduced model still maintains a nonlinear structure, due to nonlinear OCV-SOC relation and nonlinear internal heat generation. However, the electrical part of the model becomes independent since it is not affected by the thermal model. The electrical model is now upstream of the thermal model by generating resistance heat to excite the thermal model. In general, the combined online state and parameter estimation based on a nonlinear model has proven to be challenging. We propose a sequential estimation scheme to (i) estimate the core temperature and internal heat generation with a robust observer, and then (ii) design an adaptive state and parameter estimation algorithm for the electrical model by taking advantage of the estimates from the previous step.

3.1 Robust State Estimator for Thermal Model

We adopt a robust observer framework from Zhang et al. (2017) to simultaneously estimate the core temperature and internal heat generation using surface temperature measurement. The design treats the internal heat generation in the thermal model as an unknown input, and utilizes a sliding mode observer to reconstruct the unmeasured core temperature with the presence of an unknown input with a high observer gain (Khalil, 2002). Furthermore, it also produces the estimation for the unknown input which is used in subsequent designs. The robust estimation is described by the following dynamical system:

$$\frac{\mathrm{d}\hat{T}_c(t)}{\mathrm{d}t} = \frac{\hat{T}_s(t) - \hat{T}_c(t)}{R_c C_c} + L_1 \mathrm{sgn}(v), \tag{9}$$

$$\frac{\mathrm{d}\hat{T}_s(t)}{dt} = \frac{T_f(t) - \hat{T}_s(t)}{R_u C_s} - \frac{\hat{T}_s(t) - \hat{T}_c(t)}{R_c C_s} + L_2 v_s, \tag{10}$$

where $\hat{T}_c(t)$ and $\hat{T}_s(t)$ are estimates of $T_c(t)$ and $T_s(t)$, and L_1, $L_2 > 0$ are observer gains to be designed. Symbol $\mathrm{sgn}(\cdot)$ is the signum function. Moreover, $v_s = \mathrm{sgn}(T_s - \hat{T}_s)$, and v is the filtered version of $L_2 v_s$. In real time, v can be computed by passing $L_2 v_s$ through a low pass filter with unity steady-state gain, i.e. $v(t) = \{\omega/(s+\omega)\} L_2 v_s(t)$, where ω is the cut-off frequency. We now provide the convergence results of observer (9)-(10) in Theorem 1.

Theorem 1. (Zhang et al. (2017)). Consider the locally observable system (4)-(8) with heat generation $|E(t)| \leq M_E$, $\forall\, t \in \mathbb{R}^+$. If the observer gains are chosen such that

$$L_1 > \frac{M_E}{C_c} \quad \text{and} \quad L_2 > \frac{|\tilde{T}_c|_{\max}}{R_c C_s}, \tag{11}$$

where $|\tilde{T}_c|_{\max}$ is the maximum absolute value of estimation error for T_c, then the estimation error $\tilde{T}_c = T_c - \hat{T}_c$ converges to zero within finite time. In addition, the estimation of the unknown input $E(t)$ is given by

$$\hat{E}(t) = L_1 C_c \mathrm{sgn}(v). \tag{12}$$

Details can be found in Section III in Zhang et al. (2017).

3.2 Estimator for SOC and Capacity

The heat generation estimation $\hat{E}(t)$ is then utilized to algebraically compute a pseudo-measurement that decouples the measurement associated with SOC from the overall voltage. Let $y_z(t) = V_{oc}(z(t))$, and according to (6),

$$y_z(t) = V_{oc}(z(t)) = V(t) - \frac{E(t)}{I(t)}. \tag{13}$$

Since $I(t)$ and $V(t)$ are measured, $y_z(t)$ can be computed in real time by replacing $E(t)$ by its estimate $\hat{E}(t)$ (Ioannou and Sun, 2012). Hence, (1) and (13) define a new system for SOC, as follows,

$$\dot{z}(t) = \frac{1}{Q} I(t), \tag{14}$$

$$y_z(t) = V_{oc}(z(t)). \tag{15}$$

A robust observer, i.e. a sliding mode observer, is designed to simultaneously estimate SOC $z(t)$ and capacity Q:

$$\dot{\hat{z}}(t) = L_3 \mathrm{sgn}\left(y_z - \hat{y}_z\right), \tag{16}$$

$$\hat{y}_z(t) = V_{oc}(\hat{z}(t)), \tag{17}$$

where L_3 is to be designed. Under this scenario, we provide the convergence results of SOC observer (16)-(17).

Theorem 2. (Zhang et al. (2019b)). Consider the dynamical system for SOC (14)-(15), and the estimated internal heat generation from (12). Furthermore, assume $V_{oc}(z)$ is a monotonically increasing function of z over domain $0 \leq z \leq 1$. Also, assume bounds $M_I > 0, m_Q > 0$ are known, where $\left|I(t)\right| \leq M_I$, $\forall\, t \in \mathbb{R}^+$, and $Q \geq m_Q$. If the scalar observer gain L_3 verifies

$$L_3 > \frac{M_I}{m_Q}, \tag{18}$$

then the estimation error $\tilde{z}(t) = z(t) - \hat{z}(t)$ from observer (16)-(17) converges to zero in finite time. Furthermore, estimated battery capacity is given by

$$\hat{Q}(t) = -\frac{I(t)}{L_3 \mu}, \tag{19}$$

where μ is the filtered version of $\mathrm{sgn}(y_z - \hat{y}_z)$, computed by passing $\mathrm{sgn}(y_z - \hat{y}_z)$ through a low pass filter with unity steady-state gain in real time, i.e. $\mu(t) = \{\omega/(s+\omega)\}\mathrm{sgn}(y_z(t) - \hat{y}_z(t))$, where ω is the cut-off frequency.

3.3 State Estimator for ECM

The estimated heat generation $\hat{E}(t)$ is then used to calculate another pseudo-measurement to decouple the measurement associated with the R-C from the overall voltage. Let $y_e(t) = V(t) - V_{oc}(z(t))$. Now, based on (3) and (6),

$$y_e(t) = V(t) - V_{oc}(z(t)) = V_c(t) + R_1^0 I(t) = \frac{E(t)}{I(t)}. \tag{20}$$

Therefore, $y_e(t)$ can be obtained in real time by substituting $E(t)$ by its estimation $\hat{E}(t)$. Combining (2) with (20) yields the dynamical equation

$$\dot{x}(t) = -\frac{1}{R_2^0 C^0} x(t) + \frac{1}{C^0} u(t), \tag{21}$$

$$y_e(t) = x(t) + R_1^0 u(t), \tag{22}$$

where $x(t) = V_c(t)$, and $u(t) = I(t)$. Since $x(t)$ is exponentially stable when $u(t) = 0$, we design a linear Luenberger observer by injecting the estimation output error:

$$\dot{\hat{x}}(t) = -\frac{1}{R_2^0 C^0} \hat{x}(t) + \frac{1}{C^0} u(t) + L_4 \left[y_e(t) - \hat{y}_e(t)\right], \tag{23}$$

$$\hat{y}_e(t) = \hat{x}(t) + R_1^0 u(t). \tag{24}$$

The dynamics for $\tilde{x} = x - \hat{x}$ is given by

$$\dot{\tilde{x}}(t) = -\left(\frac{1}{R_2^0 C^0} + L_4\right) \tilde{x} \tag{25}$$

and $L_4 \geq -1/R_2^0 C^0$ sets the exponential convergence rate.

Remark 3. Note the parameters R_2^0 and C^0 in (23), and R_1^0 in (24). In the subsequent section we design a parameter identifier. We then formulate an adaptive observer by replacing these parameters with their estimates, via the certainty equivalence principle (Ioannou and Sun, 2012).

3.4 Parameter Identifier for ECM

In this section, we design a recursive identification algorithm for unknown ECM parameters, i.e. R_2^0 and C^0 in (23), and R_1^0 in (24), respectively. Taking Laplace transform on both sides of (21) yields

$$sX(s) - x(0) = -\frac{1}{R_2^0 C^0} X(s) + \frac{1}{C^0} U(s). \tag{26}$$

Next, take Laplace transform on both sides of (22) and substitute $X(s)$ from (26), and we have that

$$sY_e(s)-x(0)=\frac{-1}{R_2^0C^0}Y_e(s)+\frac{1}{C^0}\left(1+\frac{R_1^0}{R_2^0}\right)U(s)+R_1^0sU(s). \tag{27}$$

To avoid time differentiation, a filter needs to be applied in both sides of (27). The filter takes the form

$$\frac{1}{\Lambda(s)}=\frac{1}{(s+\lambda_1)(s+\lambda_2)}, \tag{28}$$

where λ_1 and λ_2 are time constants of the filter (Ioannou and Sun, 2012). We can derive a linear parametric model

$$Z(s)=\theta^\top\Phi(s), \tag{29}$$

where

$$Z(s)=\frac{sY_e(s)-x(0)}{\Lambda(s)}, \tag{30}$$

$$\theta=\left[-\frac{1}{R_2^0C^0}\quad \frac{1}{C^0}\left(1+\frac{R_1^0}{R_2^0}\right)\quad R_1^0\right]^\top, \tag{31}$$

$$\Phi(s)=\left[\frac{Y_e(s)}{\Lambda(s)}\quad \frac{U(s)}{\Lambda(s)}\quad \frac{sU(s)}{\Lambda(s)}\right]^\top. \tag{32}$$

Both observation Z and regressor Φ are measured or generated from measured signals. Parameter vector θ will be identified recursively. For practical implementation, the identification is formulated along with signals $z(t)$ and $\phi(t)$ in the time domain, where $Z(s)$ and $\Phi(s)$ are Laplace transform of $z(t)$ and $\phi(t)$. For instance, $\phi_3(t)$, whose Laplace transform is $\Phi_3(s)=sU(s)/\Lambda(s)$, can be obtained by computing the convolution of $u(t)$ and the inverse Laplace transform of $s/\Lambda(s)$. Hence, we avoid time differentiation of $u(t)$, which can be corrupted by noises.

With a linear parametric model, the recursive least squares algorithm is applied in an online fashion, as parameters are updated continuously

$$\dot{\hat{\theta}}=P\epsilon(t)\phi(t), \tag{33}$$

$$\epsilon(t)=\frac{z(t)-\hat{\theta}^\top\phi(t)}{m^2(t)}, \tag{34}$$

$$\dot{P}=-P\frac{\phi\phi^\top}{m^2}P,\quad P(0)=P_0 \tag{35}$$

$$m^2(t)=1+\alpha\phi^\top(t)\phi(t),\quad \alpha>0,\quad P_0=P_0^\top\succ 0 \tag{36}$$

where $\hat{\theta}$ is the estimate of θ, $\alpha>0$ is a scalar constant, and $P=P^\top\succ 0$ is a symmetric positive definite matrix. With the identified $\hat{\theta}$, the original parameters can be recovered individually by

$$\hat{R}_1^0=\hat{\theta}_3,\quad \hat{R}_2^0=-\frac{\hat{\theta}_1\hat{\theta}_3+\hat{\theta}_2}{\hat{\theta}_1},\quad \hat{C}^0=\frac{1}{\hat{\theta}_1\hat{\theta}_3+\hat{\theta}_2}. \tag{37}$$

4. ESTIMATION WITH STATE-DEPENDENT PARAMETERS

We extend the design in Section 3 to the coupled electro-thermal dynamics (1)-(8) with state-dependent electrical parameters. In fact, the parameter dependence on the states (SOC and temperature) renders the estimation task as a state-only observer design. When the state estimates have converged, the parameters can be simply retrieved assuming the map between the parameter and states are known. We will demonstrate that the methodologies from Section 3 can be readily generalized to this seemingly complex model structure with little extra efforts.

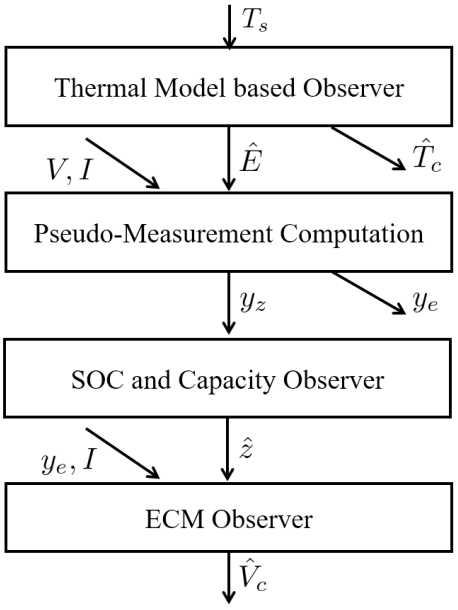

Fig. 2. Sequential observer design structure.

4.1 Estimator for Thermal, SOC, and Capacity

The first few steps essentially duplicate the estimator designs in Section 3.1 and Section 3.2. We hereby summarize these existing steps in conjunction with the design topology depicted in Fig. 2, which has four layers:

- Layer 1 – Thermal model based observer, utilizes surface temperature to estimate core temperature and heat generation. See Theorem 1.
- Layer 2 – Pseudo-measurement computation, algebraically calculates two pseudo-measurements and decouples the electrical model into two separate components. See (13)-(15) and (20)-(22).
- Layer 3 – SOC and capacity observer, estimates SOC and capacity using the pseudo-measurement of OCV, based on a sliding mode observer. See Theorem 2.
- Layer 4 – ECM observer will be discussed in detail in the subsequent section.

4.2 ECM Observer with State-Dependent Parameters

This section demonstrates the estimator design for the bottom layer of Fig. 2. The objective is to estimate the state $V_c(t)$ while taking nonlinear parameter dependence on SOC and temperature into account. We employ the reformulated model (21)-(22) and replace the constant parameters with nonlinear state-dependent parameters:

$$\dot{x}(t)=-\frac{1}{R_2(z,T,\eta)C(z,T,\eta)}x(t)+\frac{1}{C(z,T,\eta)}u(t), \tag{38}$$

$$y_e(t)=x(t)+R_1(z,T,\eta)u(t), \tag{39}$$

where $x(t)=V_c(t)$, and $u(t)=I(t)$. A state observer can be designed using linear output error injection technique,

$$\dot{\hat{x}}(t) = -\frac{1}{R_2(\hat{z},\hat{T},\eta)C(\hat{z},\hat{T},\eta)}\hat{x}(t) + \frac{1}{C(\hat{z},\hat{T},\eta)}u(t) + L_5\left[y_e(t) - \hat{y}_e(t)\right], \quad (40)$$

$$\hat{y}_e(t) = \hat{x}(t) + R_1(\hat{z},\hat{T},\eta)u(t). \quad (41)$$

Note that the estimation of SOC and temperature are injected into the above observer. Due to the sequential nature, the SOC and temperature estimators are autonomous and upstream from the state estimator for $V_c(t)$, so they are convergent independently. Theorem 4 provides the convergence analysis for the observer (40)-(41).

Theorem 4. Consider the plant model (38)-(39) and the state observer (40)-(41). If the observer gain L_5 verifies

$$L_5 > -\frac{1}{R_{2,\max}C_{\max}}, \quad (42)$$

where $R_{2,\max}$ and $C_{\max}$ denote the maximum values for $R_2(z,T,\eta)$ and $C(z,T,\eta)$, then the estimation error $\tilde{x}(t) = x(t) - \hat{x}(t)$ converges to zero exponentially.

Proof. The estimation error $\tilde{x}(t) = x(t) - \hat{x}(t)$ is described by the dynamical equation

$$\dot{\tilde{x}}(t) = -\frac{x(t)}{R_2(z,T,\eta)C(z,T,\eta)} + \frac{\hat{x}(t)}{R_2(\hat{z},\hat{T},\eta)C(\hat{z},\hat{T},\eta)} + \frac{u(t)}{C(z,T)} - \frac{u(t)}{C(\hat{z},\hat{T})} - L_5\tilde{x}(t) - L_5\left[R_1(z,T) - R_1(\hat{z},\hat{T})\right]u(t). \quad (43)$$

As $t \to \infty$, $\hat{T}(t) \to T(t)$ and $\hat{z}(t) \to z(t)$, according to Theorem 1 and Theorem 2. Hence, we have $R_1(\hat{z},\hat{T},\eta) \to R_1(z,T,\eta)$, $R_2(\hat{z},\hat{T},\eta) \to R_2(z,T,\eta)$, and $C(\hat{z},\hat{T},\eta) \to C(z,T,\eta)$, and we simplify the error dynamics for $\tilde{x}(t)$ as

$$\dot{\tilde{x}}(t) = -\left[\frac{1}{R_2(\hat{z},\hat{T},\eta)C(\hat{z},\hat{T},\eta)} + L_5\right]\tilde{x}(t). \quad (44)$$

Since $\tilde{x}(t) \in \mathbb{R}$, the estimation error $\tilde{x}(t)$ is exponentially convergent to zero if (42) is valid.

5. SIMULATION RESULTS

A simulation study is conducted on a Li-ion cell modeled using a lumped electro-thermal model (1)-(8). The state-dependent electrical parameters in (2)-(3) are taken from Lin et al. (2014). The applied current is a scaled Urban Dynamometer Driving Schedule (UDDS). The "true value" is simulated from the plant model dynamics. The simulation study is performed on two scenarios: estimation with the reduced model and with the full model.

5.1 Estimation with the Reduced Model

We first evaluate the adaptive observer in Section 3, with constant electrical parameters. The simulation results for the robust thermal state estimator are plotted in Fig. 3. The core temperature in the plant model is initialized to room temperature 25^{o}C and the estimator with a 2^{o}C initial error. According to Theorem 1, both $\hat{T}_c(t)$ and $\hat{E}(t)$ converge to their true values in finite time. Since the expression for heat generation estimate $\hat{E}(t)$ given by (12) is algebraic, the initial estimation error is proportionally

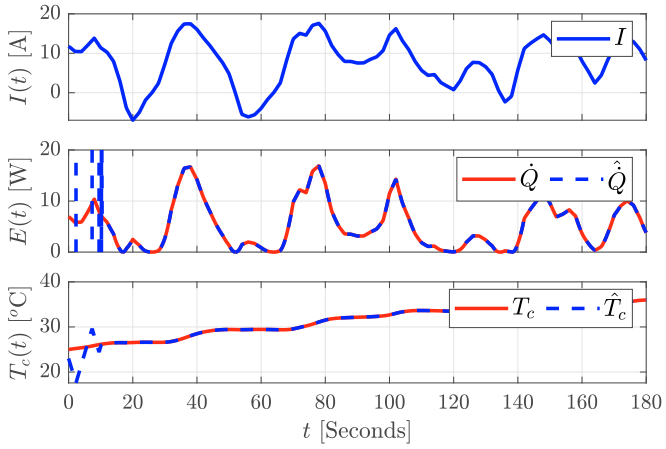

Fig. 3. Adaptive estimation for the reduced model. (a) constant electrical parameters; (b) z; (c) V_c.

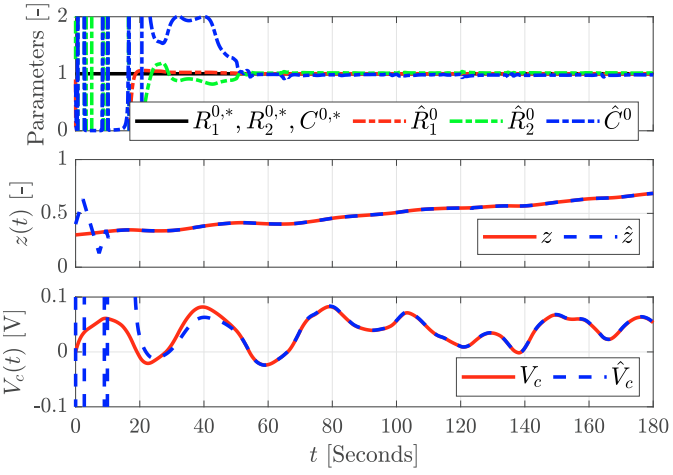

Fig. 4. Adaptive estimation for the reduced model. (a) constant electrical parameters; (b) z; (c) V_c.

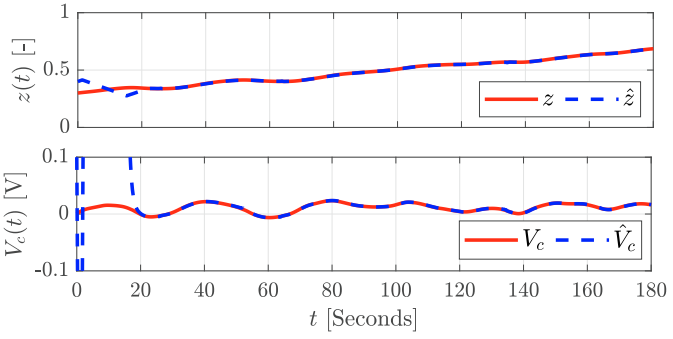

Fig. 5. Estimation results for the full model with state-dependent electrical parameters. (a) SOC; (b) V_c.

amplified by observer gain L_1. A high gain would render large initial error, as shown in the second graph in Fig. 3.

Next, the estimated $\hat{E}(t)$ is utilized to compute two pseudo-measurements in (13) and (20) for adaptive state and parameter estimation in the electrical model. As shown in Fig. 4, we recursively identify parameters R_1^0, R_2^0, and C^0 as outlined in Section 3.4. The solid black curve in Fig. 4(a) is the normalized true parameter and the dashed

curves are the parameter estimates. Even though initially the estimates experience drastic transients, the parameter estimates recover in about 50 s from large initial errors. The large initial errors are inherited from the large initial error in Fig. 3(b) and the chattering nature of the SMO. Furthermore, the SOC estimate converges in about 15 s with 10% initial error and a suitable observer gain given by (18). Finally, the capacitance voltage V_c in Fig. 4(c) obeys an exponential convergence behavior and it converges after the parameters have converged to their true values.

5.2 Estimation with the Full Model

Now consider the nonlinear state estimation with state-dependent electrical parameters. The current profile in Fig. 3(a) is used. The design follows the sequential structure depicted in Fig. 2. The first three layers overlaps with that of the previous case, as discussed in Section 4.1, so we only demonstrate the performance of the electrical state estimation. In Fig. 5, the solid curves represent the actual states whereas the dashed curve corresponds to estimates. The estimates reconstruct quickly (approximately 20 s), which verifies Theorem 4. These results confirm the convergence of nonlinear observer design based on sequential estimation scheme for a complex two-way coupled system.

6. CONCLUSION

This paper presents an adaptive estimation scheme for Li-ion batteries based on a nonlinear two-way coupled electro-thermal model, which also takes into account the dependence of electrical parameters on SOC and temperature. The design consists of four cascaded steps. A robust observer, i.e. a sliding mode observer, is utilized to simultaneously estimate the unmeasured core temperature and the unknown input heat generation. Next, the heat generation estimation is used to compute two pseudo-measurements that separates the electrical model into two components. Moreover, SOC as well as the battery capacity is then estimated. Finally, provided that temperature and SOC have converged, the capacitance voltage estimate (with time-varying parameters) is proven to converge exponentially. The results presented in this paper contribute to the existing literature in two ways: (i) designing an adaptive observer for combined state and constant parameter estimation with thermal coupling, and (ii) extending the observer design to account for state-dependent electrical parameters. These estimates are crucial for understanding the health and current operation conditions of batteries.

REFERENCES

Chaturvedi, N.A., Klein, R., Christensen, J., Ahmed, J., and Kojic, A. (2010). Algorithms for advanced battery-management systems. *IEEE Control systems magazine*, 30(3), 49–68.

Hannan, M.A., Lipu, M.S.H., Hussain, A., and Mohamed, A. (2017). A review of lithium-ion battery state of charge estimation and management system in electric vehicle applications: Challenges and recommendations. *Renewable and Sustainable Energy Reviews*, 78, 834–854.

Hu, X., Li, S., and Peng, H. (2012). A comparative study of equivalent circuit models for Li-ion batteries. *Journal of Power Sources*, 198, 359–367.

Ioannou, P.A. and Sun, J. (2012). *Robust adaptive control*. Courier Corporation.

Khalil, H.K. (2002). Nonlinear systems. *Upper Saddle River*.

Lin, X., Perez, H.E., Mohan, S., Siegel, J.B., Stefanopoulou, A.G., Ding, Y., and Castanier, M.P. (2014). A lumped-parameter electro-thermal model for cylindrical batteries. *Journal of Power Sources*, 257, 1–11.

Lotfi, N. and Landers, R.G. (2012). Robust nonlinear observer for state of charge estimation of Li-ion batteries. In *ASME 5th Annual Dynamic Systems and Control Conference joint with the JSME 11th Motion and Vibration Conference*, volume 1, 641–648.

Meng, J., Luo, G., Ricco, M., Swierczynski, M., Stroe, D.I., and Teodorescu, R. (2018). Overview of lithium-ion battery modeling methods for state-of-charge estimation in electrical vehicles. *Applied Sciences*, 8(5), 659–676.

Ning, B., Xu, J., Cao, B., Wang, B., and Xu, G. (2016). A sliding mode observer SOC estimation method based on parameter adaptive battery model. *Energy Procedia*, 88, 619–626.

Ouyang, Q., Chen, J., Wang, F., and Su, H. (2014). Nonlinear observer design for the state of charge of lithium-ion batteries. *IFAC Proceedings Volumes*, 47(3), 2794–2799.

Park, S., Zhang, D., and Moura, S. (2017). Hybrid electrochemical modeling with recurrent neural networks for Li-ion batteries. In *American Control Conference*, 3777–3782.

Plett, G.L. (2004). Extended Kalman filtering for battery management systems of LiPB-based HEV battery packs: Part 2. Modeling and identification. *Journal of Power Sources*, 134(2), 262–276.

Pop, V., Bergveld, H.J., Notten, P.H.L., and Regtien, P.P.L. (2005). State-of-the-art of battery state-of-charge determination. *Measurement Science and Technology*, 16(12), R93–R110.

Rahimi-Eichi, H., Baronti, F., and Chow, M.Y. (2013). Online adaptive parameter identification and state-of-charge coestimation for lithium-polymer battery cells. *IEEE Transactions on Industrial Electronics*, 61(4), 2053–2061.

Restaino, R. and Zamboni, W. (2012). Comparing particle filter and extended Kalman filter for battery state-of-charge estimation. In *38th Annual Conference on IEEE Industrial Electronics Society*, 4018–4023.

Wang, Y., Fang, H., Zhou, L., and Wada, T. (2017). Revisiting the state-of-charge estimation for lithium-ion batteries: A methodical investigation of the extended Kalman filter approach. *IEEE Control Systems Magazine*, 37(4), 73–96.

Zhang, D., Dey, S., Couto, L.D., and Moura, S.J. (2019a). Battery adaptive observer for a single-particle model with intercalation-induced stress. *IEEE transactions on control systems technology*.

Zhang, D., Dey, S., Perez, H.E., and Moura, S.J. (2017). Remaining useful life estimation of lithium-ion batteries based on thermal dynamics. In *American Control Conference*, 4042–4047.

Zhang, D., Dey, S., Perez, H.E., and Moura, S.J. (2019b). Real-time capacity estimation of lithium-ion batteries utilizing thermal dynamics. *IEEE Transactions on Control Systems Technology*, 28(3), 992–1000.